JOURNAL OF MATERIALS SCIENCE **40** (2005) 6499–6512

The crystallisation of Er-Si-Al-O-N B-phase glass-ceramics

Y. MENKE*
Materials and Surface Science Institute, University of Limerick, Ireland

L. K. L. FALK†
Department of Applied Physics, Chalmers University of Technology, SE-412 96, Gothenburg, Sweden

S. HAMPSHIRE
Materials and Surface Science Institute, University of Limerick, Ireland

Published online: 5 October 2005

The development of microstructure during crystallisation of a glass with composition (e/o) 35Er:45Si:20Al:83O:17N has been studied by analytical transmission electron microscopy, including electron spectroscopic imaging. The crystals take up a wide range of composition after crystallisation heat treatment at 1050 and 1150°C; the erbium cation percentage varies around that of the expected B-phase composition (Er_2SiAlO_5N), but the aluminium content is slightly lower and the silicon content higher than that. In addition, the erbium content is strongly anti-correlated with the silicon content. A comparison of B-phase composition after crystallisation of equivalent glasses formed with either yttrium, erbium or ytterbium showed that the B-phase solid solution range depends on the particular cation radius. As a consequence of this, the degree of crystallisation and the composition of the residual glass will, for equivalent glasses, also depend on the cation radius. The crystal shape is lenticular after growth at 1050°C, while heat treatment at 1150°C results in crystals with an irregular shape. In addition to crystal growth, the crystallisation heat treatment results in a phase separation of the residual glass whereby smaller silicon and nitrogen rich amorphous features form. These features are effectively pinning boundaries of growing crystals.

1. Introduction

The ability of nitrogen to substitute for oxygen in SiO_4 tetrahedral units has led to the development of a range of oxynitride glasses which are special types of silicate or alumino-silicate glasses in which some of the oxygen atoms in the tetrahedra are replaced by nitrogen, for example, as in SiO_3N [1–8]. Oxynitride glass-forming regions are essentially extensions of the oxide glass-forming regions [1, 2, 8, 9]. The substitution of nitrogen for oxygen enables, in many cases, oxynitride glass formation where it is not possible, or very difficult, to form equivalent oxide glasses [1, 2]. The substitution of small to moderate amounts of nitrogen for oxygen generally leads to a lower glass melting temperature (T_m), an increased melt viscosity and an inhibition of the nucleation of pure silicate phases from these melts or glasses [1].

A number of studies have addressed the formation of multi-phase glass-ceramics in yttrium and rare earth Si-Al-O-N systems [10, 11]. It is only recently, however, that appropriate combinations of glass composition and crystallisation heat treatment for the formation of just one crystalline, five-component, phase have been established. These glass-ceramics contain either the so-called B-phase, or the related high temperature phase I_w [12–16].

B-phase has a hexagonal structure of symmetry $P6_3/m$ with lattice parameters of $a = 3.8359$ Åand $c = 9.7539$ Å[17, 18]. It has been proposed that the yttrium B-phase structure is a bi-dimensional network of randomly linked $(Si,Al)(O,N)_4$ tetrahedra between layers of yttrium cations. The composition of B-phase is thought to lie on the $YSiO_2N$–$YAlO_3$ tie line, and to have a solid solution range of 40–70 mol% $YAlO_3$ [19]. The proposed stoichiometric mid-point composition is Y_2SiAlO_5N [19].

B-phase glass-ceramics can be easily formed in the Y-SiAlON system through crystallisation of a

Present Address: Politecnico di Torino, Dipartimento di Scienza dei Materiali ed Ingeneria Chimica, C.so Duca degli Abruzzi, 24, 10129, Torino, Italy.
†Author to whom all correspondence should be addressed.

0022-2461
DOI: 10.1007/s10853-005-2151-0

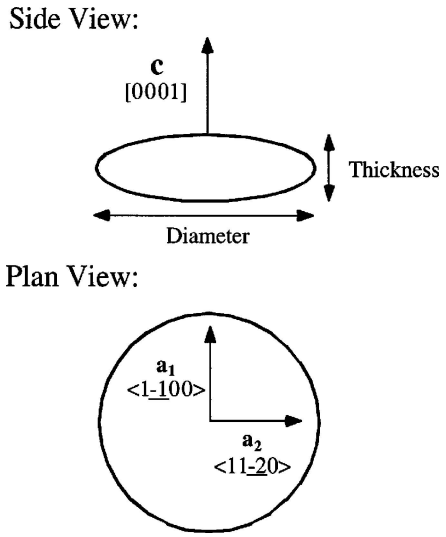

Figure 1 The relationship between the lenticular B-phase crystal shape and the hexagonal lattice. After Young *et al.* [14].

nitrogen rich, 17 equivalent % (e/o)[1], parent glass with an Y:Si:Al ratio in e/o of 35:45:20 at temperatures in the range 965 to 1050°C. A typical B-phase glass-ceramic microstructure formed in the Y-SiAlON system consists of lenticular crystals of B-phase surrounded by a residual glassy phase [13, 14]. Detailed imaging and electron diffraction in the transmission electron microscope (TEM) showed that there is a relationship between the shape of freely growing crystals and the hexagonal B-phase lattice. The crystals grow preferentially parallel to the basal plane of the hexagonal structure to form a lenticular shape with the *c*-axis of the hexagonal lattice in the direction of the axis of the lenticular crystal, see Fig. 1 [14].

The ionic radii of the high atomic number rare-earths (e.g. Dy^{3+}, Er^{3+} and Yb^{3+}) are very close to that of Y^{3+}, and, therefore, B-phase should crystallise also from the equivalent glass prepared in a high atomic number rare-earth SiAlON system. In one study, it was found that two completely different phase assemblages emanate from a glass of composition (e/o) 35Er:45Si:20Al:83O:17N when heat treated for 10 h below or above 1190°C [15]. X-ray diffraction showed that B-phase was the only crystalline product at temperatures below 1190°C whereas Er-N-apatite, Er-Al-garnet and β-$Er_2Si_2O_7$ formed in addition to B-phase during crystallisation at higher temperatures.

The aim of the present work was to examine the development of microstructure during nucleation and crystallisation heat treatments of a parent glass of composition (e/o) 35Er:45Si:20Al:83O:17N. The glass was crystallisation heat treated at temperatures where B-phase was expected to form. The fine scale microstructures were characterised by different transmission electron microscopy techniques, including electron spectroscopic imaging, and special attention was paid to the chemical composition of crystals and residual glass.

[1]The calculation of compositions in equivalent % (e/o) is described in detail in reference [5].

2. Experimental procedures

2.1. Glass preparation

The Er-Si-Al-O-N glass was prepared from a mixture of silicon nitride and high purity oxides: Er_2O_3, Al_2O_3, and SiO_2. The oxide powders were calcined at 900°C to remove any volatiles or chemically absorbed water. The atomic composition of the starting powder mixture was 15.2% erbium, 14.7% silicon, 8.7% aluminium, 54.1% oxygen and 7.4% nitrogen, which corresponds to an overall composition in e/o of 35Er:45Si:20Al:83O:17N. The Si_3N_4 powder contained 1.4 wt% O, corresponding to 2.625 wt% SiO_2, and this was accounted for in the preparation of the starting powder mixture.

The mixed powders were wet ball milled in 2-Propanol with β-SiAlON for 10 h, followed by evaporation of the alcohol before compacting into pellets (∼50 g) in a cold isostatic press. The pellets were placed in a boron nitride lined graphite crucible and melted for 1 h at 1715°C under flowing nitrogen at ∼0.1 MPa in a vertical tube furnace. After rapid removal from the hot zone, the melt was poured into a preheated (900°C) graphite mould, annealed at 850°C for 1 h in order to release internal stresses, and then slowly cooled in the annealing furnace to room temperature.

2.2. Heat treatment

The optimum nucleation temperature for Er B-phase glass-ceramics has previously been determined as 948°C [20]. In order to reveal the influence of the nucleation heat treatment on crystal development, samples were either heated directly to the crystallisation temperature 1050 or 1150°C, or held for 3 or 50 h at the nucleation temperature prior to heating to 1050°C. The 50 h nucleation heat treatment was then followed by 1 h at 1050°C, while specimens held for 3 h at 948°C were held for 1 or 10 h at 1050°C in order to study crystal development during prolonged heat treatment. In addition, one sample was characterised after a 50 h nucleation heat treatment. The different nucleation and crystallisation heat treatments are summarised in Table I.

The heat-treatments were carried out in a horizontal tube furnace with the glass specimens embedded in boron nitride in alumina boats. The heating rate was 10°C/min, and the specimens were cooled in the furnace at 10°C/min after heat treatment. Measures were taken to ensure that oxygen and water vapor were eliminated from the furnace before the samples were heated to the nucleation or crystallisation temperature, and all heat treatments were performed under flowing nitrogen.

2.3. Microstructural characterisation

2.3.1. X-ray diffraction and scanning electron microscopy

The quality and homogeneity of produced glass and glass-ceramics were assessed by powder X-ray diffraction (XRD) and scanning electron microscopy (SEM). Samples for XRD were prepared by crushing in a gyro mill with a boron carbide liner. Smaller amounts of KCl were added as an internal standard, and the powdered

TABLE I Heat treatments carried out for observation of crystal nucleation and growth together with the average values of the lenticular crystal diameter (d) and thickness (t). The differences in these average values between the different materials crystallisation heat treated at 1050°C are given as the deviation from d_m and t_m, where d_m and t_m are the mean values of the average diameter and thickness, respectively, after heat treatment at 1050°C

		Crystal size				
Nucleation	Crystallisation	d (nm)	$(d-d_m)/d_m$ (×100%)	t (nm)	$(t-t_m)/t_m$ (×100%)	d/t
948°C, 50 h	–	165	–	55	–	3.0
948°C, 50 h	1050°C, 1 h	459	3.6	107	−18	4.6
948°C, 3 h	1050°C, 1 h	440	−0.68	107	−18	4.1
948°C, 3 h	1050°C, 10 h	432	−2.9	139	6.5	3.2
–	1050°C, 10 h	441	−0.45	169	30	2.8
–	1150°C, 10 h	531	–	–	–	–

specimens were characterised using an X-ray powder diffractometer with Cu K_α radiation. Traces were compared with standards from the ICDD database and XRD data from relevant publications [20] in order to identify the crystallisation products.

Glass homogeneity and the overall structure after nucleation and crystallisation heat treatments was assessed by SEM of polished and gold sputter-coated sections.

2.3.2. Transmission electron microscopy

Thin foil specimens for transmission electron microscopy (TEM) were prepared by a standard method for ceramic materials. Thin slices (500–600 μm) were cut with a diamond saw. These were then polished, on both sides, to a thickness of approximately 100 nm. Disks 3 mm in diameter were cut with an ultrasonic drill, and the disks were dimpled to a minimum thickness of around 30 nm. The dimpled disks were ion beam thinned to perforation using 5 kV argon ions incident on both sides at angles between 5 and 10°. A carbon film (nominal thickness of 4 nm) was evaporated onto one side of the perforated disk in order to prevent charging under the electron beam in the TEM.

The thin foils were then characterised in a field emission transmission electron microscope (FEG-TEM)[2] operating at 200 kV and equipped with a system for energy dispersive X-ray spectroscopy (EDX)[3] and a post-column imaging filter (GIF).[4]

The cation composition (cation %) of crystals and residual glass was determined by EDX point analysis using an electron probe with a nominal FWHM of around 1 nm. Elemental profiles acquired by the EDX system attached to the FEG-TEM were used for the evaluation of peak areas in the quantitation of the EDX spectra. Nitrogen/oxygen ratios of the crystalline and amorphous phases in one of the specimens (nucleation heat treated for 3 h at 948°C followed by 1 h at 1050°C) were determined by electron energy loss spectroscopy (EELS) using the GIF and the EL/P software with Hartree-Slater cross sections. The EEL spectra were collected in diffraction mode to ensure that the area of analysis was well defined. Simultaneous acquisition of EDX and EEL spectra from the same volume made it possible to correlate anion ratios to cation ratios. The results from all EDX and EELS analyses were also converted to e/o according to the formulae in reference [5].

Estimates of the residual glass content after crystallisation heat treatments were made from dark field images formed using part of the diffuse scattering from the glass [14]. These dark field images were scanned and converted to binary. The threshold level was adjusted so that the crystals appeared black, while the glass appeared white. Since the crystals appeared to be both randomly distributed and randomly oriented on a scale of a few micrometers, the area fraction of a thin section containing several crystals (i.e. a low magnification TEM image) was assumed to be equal to the volume fraction of the bulk.

Crystal sizes and shapes were estimated from measurements of the maximum Feret diameter (F_m), and the Feret diameter perpendicular to F_m (F_p), of crystal sections in TEM images.

Combined analytical and spatial information was obtained from electron energy filtered images [21–23]. These images were recorded around the nitrogen K, oxygen K, aluminium $L_{2,3}$ and erbium $N_{4,5}$ edges in the EEL spectrum. An energy selecting slit width of 20 eV was used for the acquisition of pre- and post-edge images around the nitrogen K, aluminium $L_{2,3}$ and erbium $N_{4,5}$ edges, while a 40 eV slit was used for the pre- and post-edge images around the oxygen K edge. Elemental distribution images for oxygen, aluminium and erbium were displayed as the jump ratio between a post-edge and a pre-edge image, and for nitrogen as the edge intensity versus position in the microstructure. A brighter contrast in the calculated images reflects a higher concentration of the particular element.

3. Results

3.1. The phase composition of nucleated and crystallised glass

XRD and selected area electron diffraction in the TEM showed that the nucleation and crystallisation heat treatments of the glass, carried out according to Table I, resulted in one crystalline, five-component, phase that was unambigously identified as B-phase. Acquired electron diffraction patterns were consistent

[2]Philips CM200 SuperTwin.
[3]Oxford Instruments super-ATW detector and the Link Isis software.
[4]Gatan Imaging Filter (GIF).

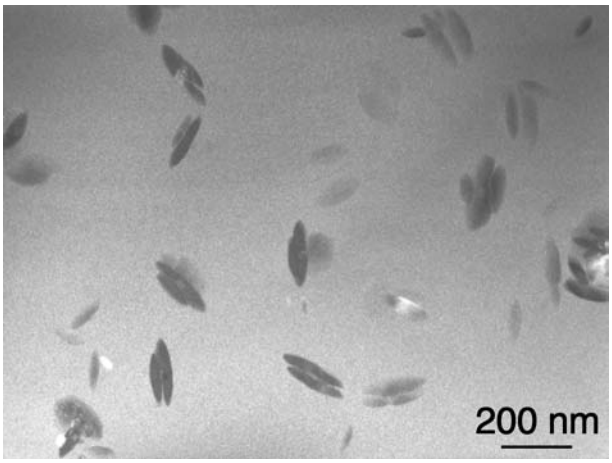

Figure 2 The glass-ceramic structure after nucleation heat treatment at 948°C for 50 h showing crystals with elongated and rounded cross-sections dispersed in a matrix of residual glass. TEM centered dark field image formed from part of the diffuse scattering from the residual glass.

with electron diffraction data previously obtained for yttrium B-phase [14].

3.2. Stuctural development during long term nucleation heat treatment

Heat treatment for 50 h at the nucleation temperature 948°C resulted in a limited nucleation and growth of lenticular crystals, see Figs. 2 and 3. The volume fraction of residual glass was estimated to be ~93%. The crystal morphology was the same as observed previously during nucleation and early growth of Y B-phase; elongated as well as rounded crystal cross-sections were observed. The average crystal diameter and thickness (see Fig. 1) were estimated from measurements of F_m and F_p, respectively, on the lenticular crystal cross-sections. This gave an average crystal diameter of 165 nm and an average thickness of 55 nm (Table I). The crystals appeared in pairs, or in groups, around crystalline features that were shown by EDX to be rich in silicon but devoid of erbium and aluminium, see Fig. 3. Similar silicon-rich crystals have been observed previously in yttrium B-phase glass, where they served as heterogeneous nucleation sites for B-phase crystals during nucleation and crystallisation heat treatments [14].

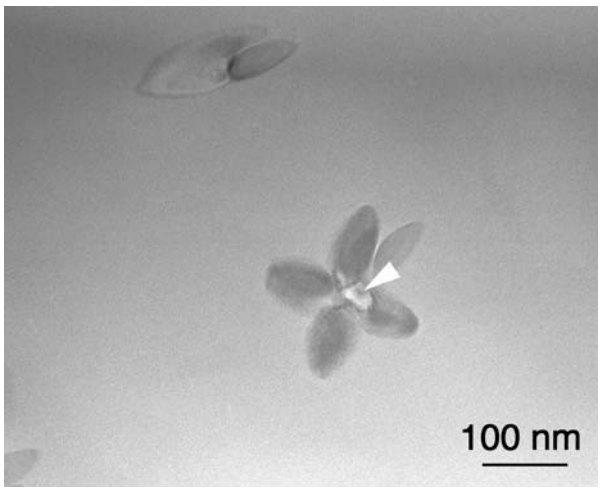

Figure 3 Group of crystals surrounding a silicon-rich crystalline feature (arrowed) after nucleation heat treatment at 948°C for 50 h.

There was a certain spread in the composition of crystals and residual glass after nucleation heat treatment, see Figs 4a and 5a. The crystals had a comparatively high silicon content, and their erbium and aluminium contents decreased with increasing silicon content. The average cation composition of the crystals was (cation %) 40 ± 5 Er, 42 ± 3 Si and 18 ± 2 Al, and that of the residual glass was (cation %) 38 ± 4 Er, 41 ± 3 Si and 21 ± 3 Al (Table II). The average compositions converted to e/o are given in Table III.

3.3. Crystal growth

3.3.1. Nucleation heat treatment followed by crystallisation heat treatment

Crystallisation heat treatment at 1050°C for 1 h following a nucleation treatment for 50 h resulted in an increased density of crystals and a significantly reducted residual glass content; the volume fraction of residual glass in this specimen had decreased to around 35%, see Table II and Fig. 6. The average crystal section diameter had increased to 459 nm and the thickness to 107 nm (Table I). The crystals were often present in groups surrounding a silicon-rich crystal. Computation of elemental distribution images showed that the central crystal was also depleted in oxygen, apart from erbium and aluminium, see Fig. 7.

The time at temperature during nucleation heat treatment at 948°C did not have any obvious effects on the overall microstructure. A nucleation treatment for 3 h preceeding the 1 h crystallisation heat treatment at 1050°C resulted in a glass-ceramic with a high density of crystals and a residual glass volume fraction of 35% (Table II). The lenticular crystals were also in this case often present in groups around crystalline silicon-rich features. The apparent crystal size, as revealed by the crystal section measurements, was virtually the same as after the longer nucleation heat treatment (Table I).

A prolonged heat treatment (10 h) at 1050°C following a 3 h nucleation heat treatment resulted in a significant reduction of the residual glass content; this sample had a residual glass volume fraction of around 24% (Table II). The crystal section measurements indicated that also the crystal shape changed with time at temperature; the average crystal section thickness had increased significantly (around 30%), while the average diameter was virtually the same as after the shorter crystallisation heat treatment, see Table I.

3.3.2. Crystallisation heat treatment without nucleation

The residual glass content was virtually the same (25%; see Table II) after 10 h heat treatment at 1050°C without a preceeding nucleation treatment. The 3 h nucleation heat treatment at 948°C seemed, however, to have an effect on the crystal shape after 10 h at 1050°C, see Table I and Fig. 8. The average crystal section thickness was larger in the specimen that had not undergone nucleation, while the average crystal section diameter was virtually the same.

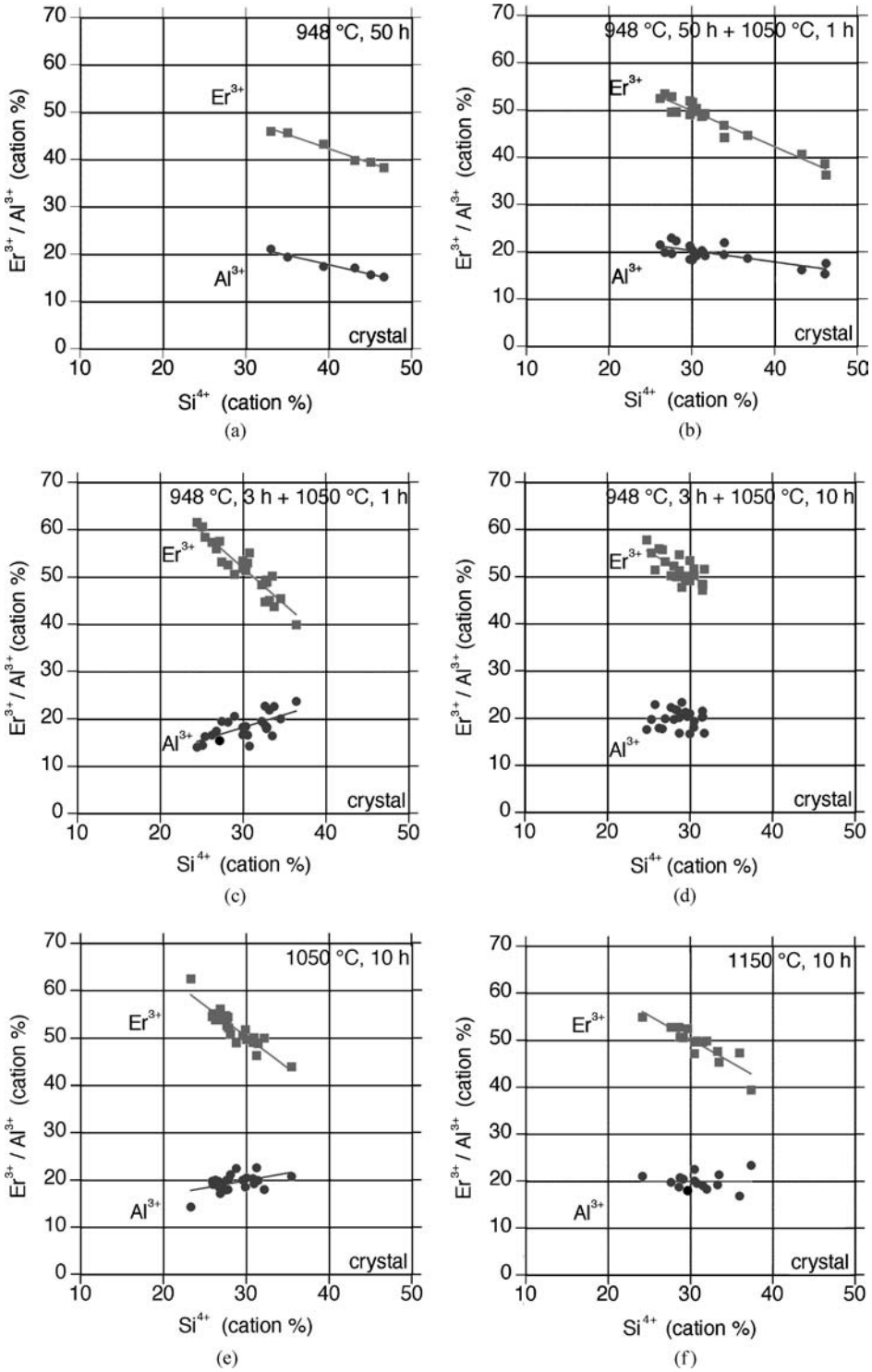

Figure 4 Variation in the cation contents of the crystals in the different samples. The data points are based on individual EDX point analysis, and the errors are typically less than 5%. The lines are drawn for visual reference only.

TABLE II Glass contents determined from dark field images and average cation compositions from EDX for the B-phase crystals and the residual glass for each sample

		Crystal composition (cat%)			Glass composition (cat%)		
Sample	Glass content (%)	Er	Si	Al	Er	Si	Al
948°C (50 h)	93	40 ± 5	42 ± 3	18 ± 2	38 ± 4	41 ± 3	21 ± 3
948°C (50 h) + 1050°C (1 h)	35	48 ± 5	33 ± 6	20 ± 2	27 ± 5	49 ± 6	24 ± 3
948°C (3 h) + 1050°C (1 h)	34	52 ± 6	30 ± 3	18 ± 3	27 ± 6	54 ± 8	19 ± 5
948°C (3 h) + 1050°C (10 h)	24	51 ± 3	29 ± 2	20 ± 2	27 ± 3	47 ± 4	26 ± 3
1050°C (10 h)	25	52 ± 4	29 ± 3	19 ± 2	32 ± 10	44 ± 9	24 ± 4
1150°C (10 h)	26	49 ± 4	31 ± 3	20 ± 2	30 ± 5	40 ± 3	30 ± 3

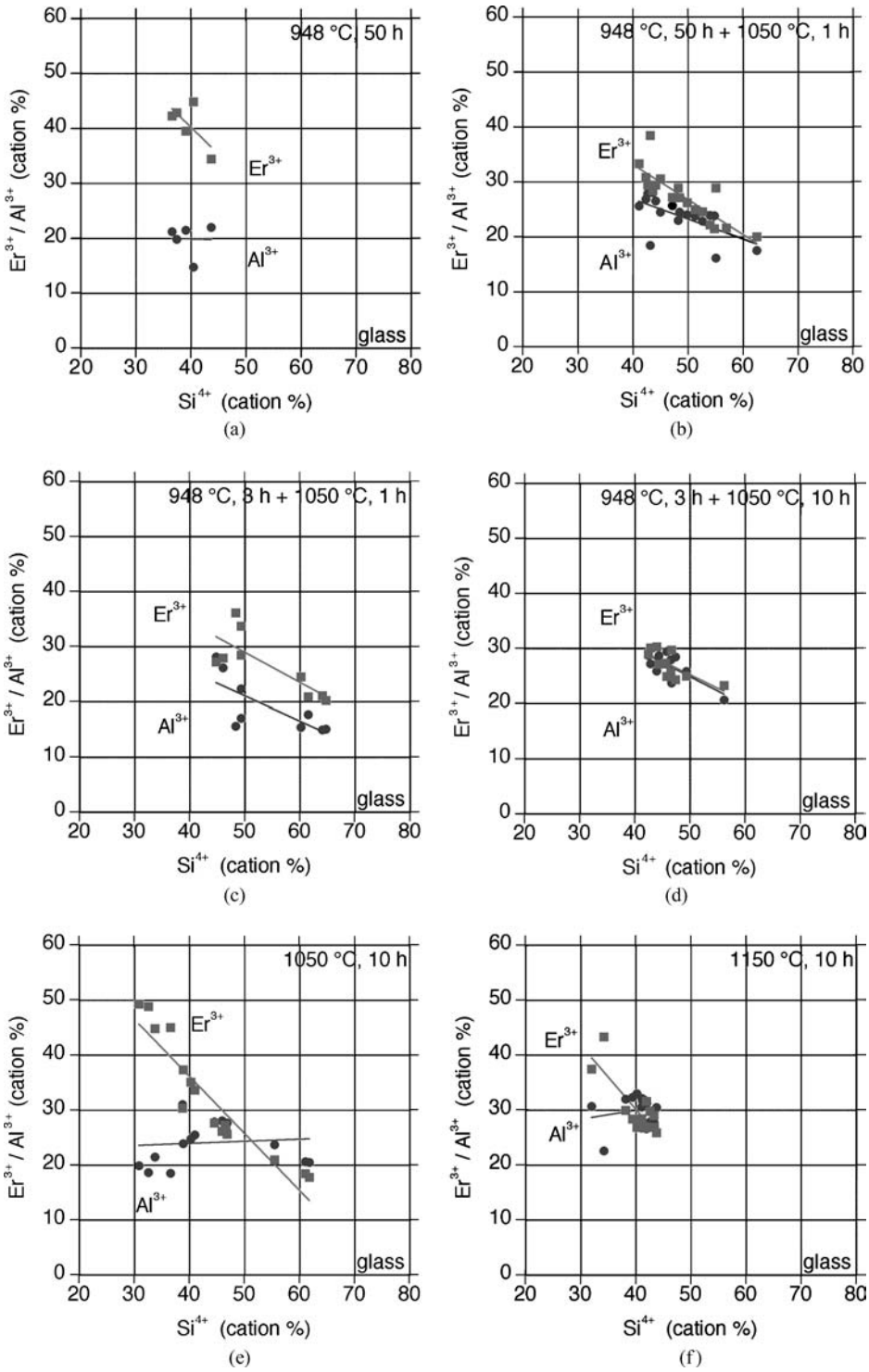

Figure 5 Variation in the cation contents of the residual glass in the different samples. The data points are based on individual EDX point analysis, and the errors are typically less than 5%. The lines are drawn for visual reference only.

TABLE III Average compositions in e/o of crystals and residual glass calculated from the average compositions in cation % shown in Table II

	Crystal composition (e/o)			Glass composition (e/o)		
Sample	Er	Si	Al	Er	Si	Al
948°C (50 h)	35.1	49.1	15.8	33.4	48.1	18.5
948°C (50 h) + 1050°C (1 h)	42.9	39.3	17.9	23.2	56.2	20.6
948°C (3 h) + 1050°C (1 h)	47.3	36.4	16.4	22.9	61.0	16.1
948°C (3 h) + 1050°C (10 h)	46.5	35.3	18.2	23.3	54.2	22.5
1050°C (10 h)	47.4	35.3	17.3	27.9	51.2	20.9
1150°C (10 h)	44.4	37.5	18.1	26.5	47.0	26.5

Increasing the crystallisation heat treatment temperature to 1150°C did not have any effect on the degree of crystallisation, see Table II. The sample held for 10 h at this temperature (without preceeding nucleation treatment) had a residual glass volume fraction of around 26%. The grain morphology was, however, quite different in this sample. The crystals had an irregular shape with an average section diameter of 531 nm, see Fig. 9, and elongated crystal cross-sections were not observed.

3.4. Glass morphology after crystallisation heat treatment

The glass residue after crystallisation heat treatment contained smaller features that appeared with brighter contrast than the surrounding glass in bright field TEM images, see Fig. 10. They were shown by electron diffraction and substantial tilting to be amorphous, and they often had a "flowery" appearance. EDX analysis showed that these features were much more silicon-rich than either the crystals or the residual glassy phase. The density of these silicon-rich and amorphous features increased with time at 1050°C, and they also seemed to have an effect on crystal growth. As shown in Fig. 10, these features were very effective in pinning boundaries of growing crystals, which would reduce crystal growth rate and the resulting crystal size.

3.5. Elemental compositions after crystallisation heat treatment

3.5.1. Electron spectroscopic imaging

The elemental distribution images calculated from acquired electron energy filtered images clearly showed that the crystals had higher erbium, aluminium and oxygen contents, but a lower nitrogen content, than the residual glass, see Fig. 11. The computation of the erbium jump ratio image in Fig. 11 is shown in Fig. 12. Two electron spectroscopic images were recorded with a 20 eV energy selecting slit centered around energy losses of 158 eV (pre-edge image) and 178 eV (post-edge image). The erbium jump ratio map was then calculated by dividing the post-edge image by the pre-edge image.

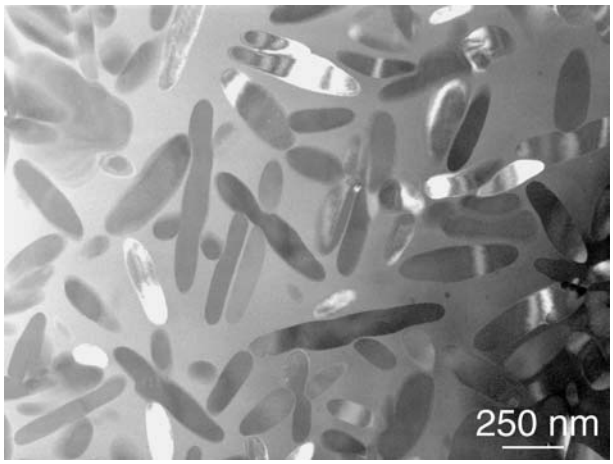

Figure 6 The glass-ceramic structure after crystallisation heat treatment at 1050°C for 1 h following nucleation heat treatment at 948°C for 50 h. TEM centered dark field image formed from part of the diffuse scattering from the residual glass.

Calculated elemental distribution images also showed that the silicon rich amorphous features that formed in the residual glass during crystallisation heat treatment at 1050°C were depleted in erbium and aluminium, but enriched in nitrogen, see Fig. 11.

3.5.2. Elemental analysis of crystals and residual glass

A substantial range of composition was clearly present for the crystals after crystallisation heat treatment. Crystal growth at 1050°C was associated with an adjustment of crystal composition towards lower silicon and higher erbium contents, see Fig. 4. In all cases the erbium concentration was clearly anti-correlated with the silicon content.

The specimen that had been nucleated for 50 h and subsequently held for 1 h at 1050°C still showed an aluminium concentration that decreased slightly with increasing silicon content. Nucleation for 3 h followed by 1 h at 1050°C showed, however, a clear correlation between aluminium and silicon; an increased silicon content was associated with an increase in the aluminium concentration. A slight increase in aluminium with an increased silicon content was also observed after prolonged heat treatment (10 h), see Fig. 4d).

The crystals in the samples heated directly to the crystallisation temperatures of 1050 or 1150°C and held there for 10 h had very similar ranges of composition, see Figs 4e and 4f. The erbium concentration was, again, clearly anti-correlated with the silicon content, and there was a slight increase in the aluminium content with an increasing silicon concentration.

The mean and standard deviation of the measured compositions of the crystals and the residual glass for each material are listed in Table II. The average composition of the crystals in the samples subjected to a crystallisation heat treatment at 1050 or 1150°C are remarkably similar, and an overall average cation composition was calculated of (cation %) 51 ± 4 Er, 30 ± 3 Si, and 19 ± 2 Al. This suggests that the stoichiometric composition of B-phase is close to this composition, which can be rationalised in atomic ratios as Er:Si:Al = 5:3:2.

The residual glass in all specimens showed a wide range of composition but was clearly leaner in erbium and richer in silicon than the crystals, as also demonstrated by the computed elemental distribution images, see Fig. 11. Both erbium and aluminium appeared to be anti-correlated with silicon. A prolonged heat treatment at 1050°C seemed to reduce the spread in composition, as did the 3 h nucleation heat treatment at 948°C, see Fig. 5. The average residual glass compositions were fairly similar after the different crystallisation heat treatments at 1050 or 1150°C, see Table II, although with a little variability from one specimen to another. An average cation composition from all crystallised samples was calculated as (cation %) 29 ± 7 Er, 46 ± 8 Si, and 25 ± 5 Al. This is leaner in erbium but richer in silicon than the residual glass in the sample that had been nucleation heat treated at 948°C for 50 h, which is consistent with the adjusted crys-

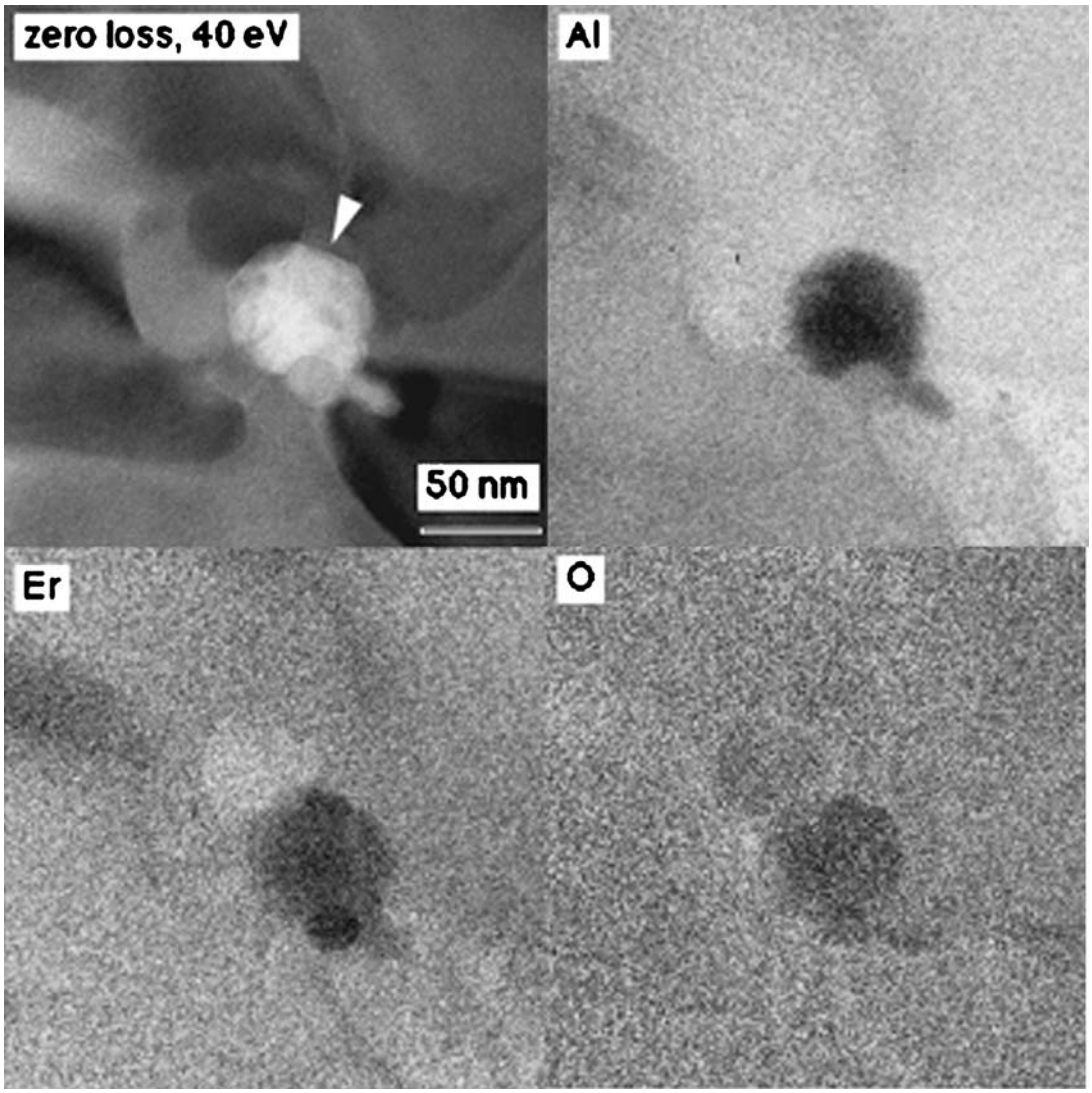

Figure 7 Zero loss and elemental distribution images of a crystalline silicon-rich feature (arrowed) surrounded by B-phase crystals. This sample was crystallisation heat treated at 1050°C for 1 h after nucleation heat treatment at 948°C for 50 h.

tal composition after crystallisation heat treatment, see Table II.

The range of B-phase crystal cation composition in the samples crystallisation heat treated at 1050 and 1150°C, as converted to e/o, is shown on the triangular section (constant O/N ratio) of the Jänecke prism in Fig. 13. The average cation compositions of the crystals and the residual glass after conversion to e/o are given in Table III.

The results from the simultaneous EDX and EELS analysis of the specimen held for 3 h at 948°C followed by 1 h at 1050°C gave an average cation composition of (cation %) 46.1 ± 3.5 Er, 34.5 ± 3.1 Si and 19.5 ± 1.7 Al for the crystals, which is well within the composition range shown in Fig. 4c. The corresponding average anion composition (anion %) was 96.0 ± 2.6 O and 4.0 ± 2.3 N. This gives an average normalised formula for the crystals of $Er_5Si_{3.8}Al_2O_{17}N_{0.75}$. The combined analysis of the residual glass gave for the cations (cation %) 28.2 ± 1.0 Er, 47.7 ± 1.0 Si and 28.1 ± 1.1 Al, again well within the compositional range shown in Fig. 5c, and for the anions (anion %) 91.3 ± 3.8 O and 8.7 ± 2.3 N. This gives an average normalised formula for the residual glass of $Er_2Si_{3.1}Al_2O_{10.7}N$. These average normalised formulae for the B-phase crystals and the residual glass were also converted to e/o. This gave an average crystal composition of (e/o) 41Er:42Si:17Al:94O:6N and an average glass composition of (e/o) 25Er:50Si:25Al:88O:12N.

4. Discussion

This work has demonstrated that the crystallisation of the glass (e/o) 35Er:45Si:20Al:83O:17N at temperatures up to 1150°C results in a single phase glass-ceramic with a microstructure that initially consists of groups of lenticular B-phase crystals surrounded by a residual glass. Although this microstructure is very similar to that which forms during crystallisation of the equivalent yttrium SiAlON glass [14], there are a number of distinct differences between the two glass-ceramic microstructures. The choice of cation has an effect, not only on the optimum nucleation temperature (965°C for yttrium B-phase and 948°C for erbium B-phase), but also on the range of crystal composition, the degree of crystallisation as well as the extent of phase separation in the residual glass, and, finally, B-phase crystal size and shape. This will be discussed below.

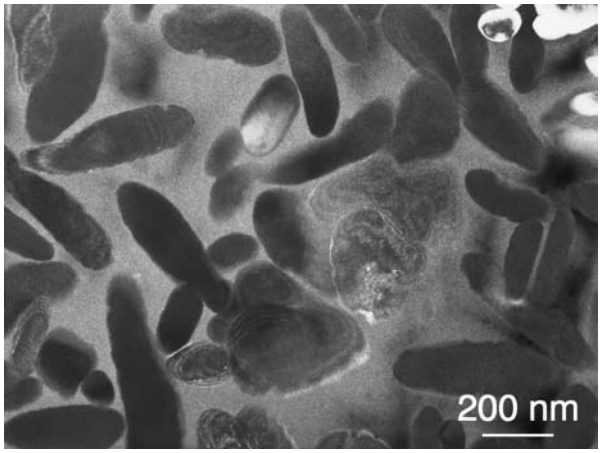

Figure 8 The glass-ceramic structure after crystallisation heat treatment at 1050°C for 10 h without preceeding nucleation heat treatment. TEM centered dark field image formed from part of the diffuse scttering from the residual glass.

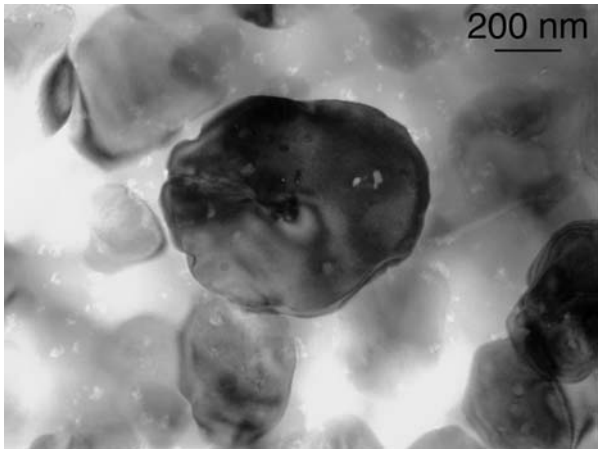

Figure 9 The glass-ceramic structure after crystallisation heat treatment at 1150°C for 10 h without preceeding nucleation heat treatment.

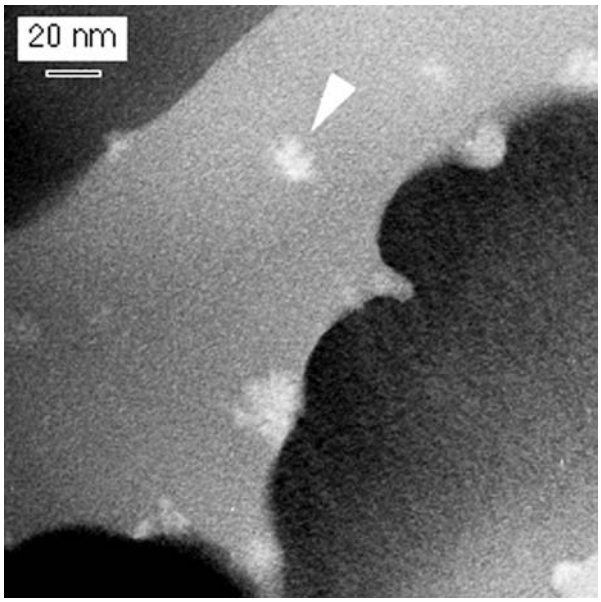

Figure 10 Silicon-rich amorphous features (arrow) that formed from the residual glass during prolonged crystallisation heat treatment at 1050°C. These features seemed to pin crystal boundaries resulting in un-even crystal surfaces.

4.1. Composition

The erbium B-phase crystals took up a substantial range of composition, and the erbium was clearly anti-correlated with the silicon, see Fig. 4. A slight decrease in the aluminium content with increasing silicon content was observed for the two samples that had been nucleation heat treated for 50 h. The crystals in the other samples showed, however, no pronounced variation in the aluminium content or, in some cases, a slight increase with increasing silicon content. These results suggest that, in addition to the random substitution of silicon by aluminium in the (Si,Al) $(O,N)_4$ tetrahedra, a locally increased density in the bi-dimensional network of randomly oriented tetrahedra is associated with an increased density of vacancies in the erbium lattice.

The same behaviour has been observed for yttrium, ytterbium, and yttrium + ytterbium B-phase crystals [14, 24, 25]. The range of the B-phase composition is, however, dependent upon the cation radius as shown in Fig. 14. The smallest cation Yb^{3+}, $r(Yb^{3+}) = 0.868$ Å, results in a comparatively high content of ytterbium with a solid solution range around an average value of 62.4 cation %, while the significantly larger Y^{3+}, $r(Y^{3+}) = 0.893$ Å, gives a solid solution range around an average of 47.2 cation % [14, 24]. The solid solution range for erbium, $r(Er^{3+}) = 0.880$ Å, in the erbium B-phase structure is in between; the average erbium content determined in the present investigation is 51.0 cation %. As a consequence of the anti-correlation with silicon, the silicon solid solution range will go to higher values as the ytterbium is replaced by erbium or yttrium, see Fig. 14. It seems, thus, that the cation lattice becomes more densely occupied when the cation radius is reduced, and as a consequence of that, the bi-dimensional network of randomly linked (Si,Al) $(O,N)_4$ tetrahedra becomes more open. The proposed stoichiometric mid-point composition (Y_2SiAlO_5N) and solid solution range of yttrium B-phase from reference [19] are also included in Fig. 14. The data in Fig. 14 demonstrates that the average cation composition of the erbium B-phase crystals coincides with the end point composition (70 vol% $YAlO_3$) of the proposed solid solution range for yttrium B-phase. The yttrium B-phase composition falls, however, outside this range, and so does the average ytterbium B-phase composition.

The combined EDX and EELS analyses indicated an average formula of $Er_5Si_{3.8}Al_2O_{17}N_{0.75}$ for erbium B-phase. The EELS analyses showed, hence, that the B-phase crystals were less nitrogen-rich than what has previously been proposed for yttrium B-phase [19]. The proposed stoichiometric composition, Y_2SiAlO_5N, has a nitrogen:oxygen ratio of 0.2, while the EELS measurements in the present investigation gave an average anion ratio of 0.04. This has further implications on the structure of B-phase; the randomly linked (Si,Al) $(O,N)_4$ tetrahedra are comparatively rich in aluminium, see Fig. 14, but have a very low nitrogen content. This indicates that B-phase is almost an oxide phase, as has previously been suggested for the related monoclinic high temperature phase I_w [26].

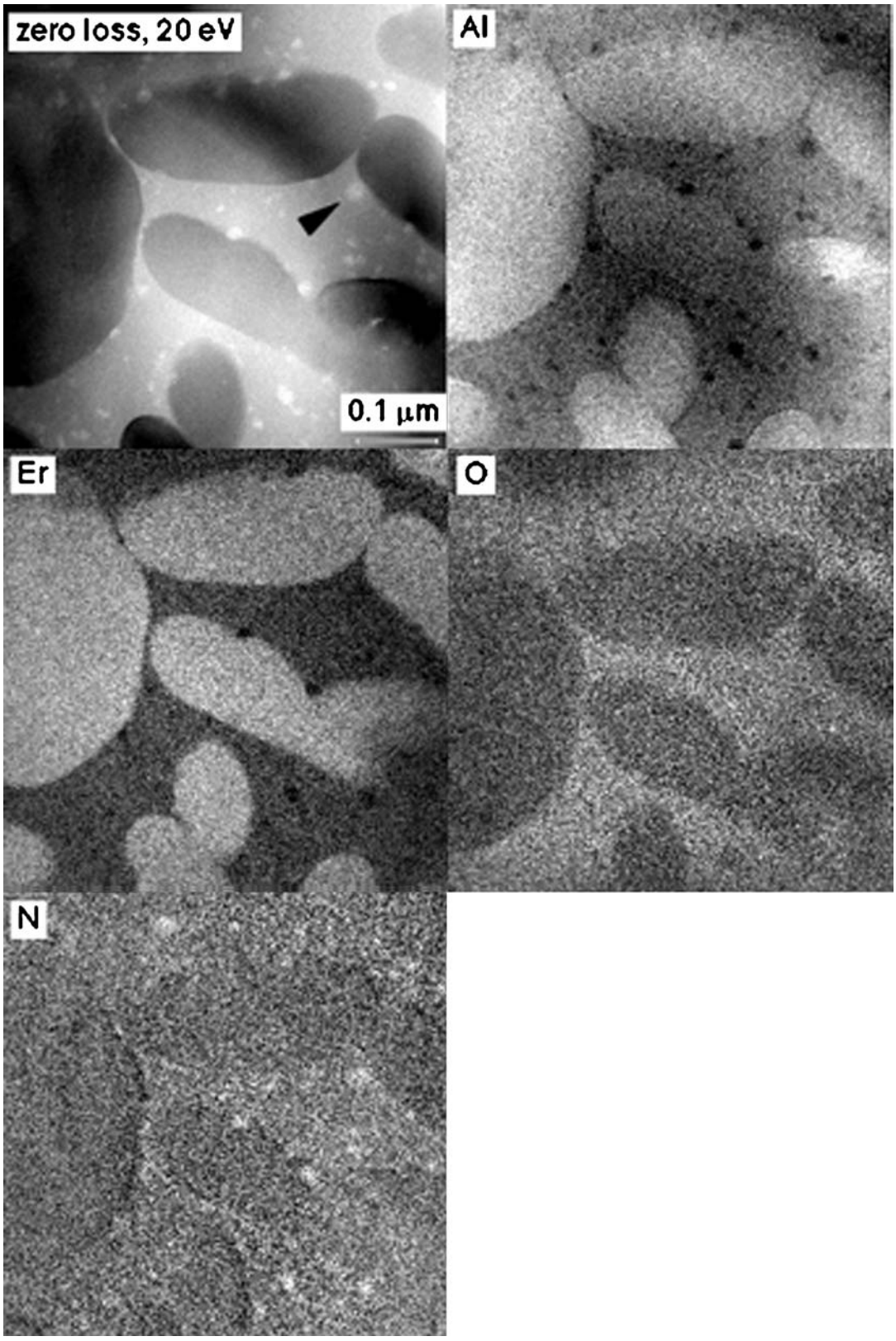

Figure 11 Zero loss and calculated elemental distribution images of the glass-ceramic that had been crystallisation heat treated at 1050°C for 10 h after nucleation heat treatment at 948°C for 3 h. Silicon- and nitrogen-rich amorphous features (arrow in zero loss image) separated from the glass during crystallisation heat treatment.

4.2. Degree of crystallisation and extent of residual glass phase separation

The composition range of B-phase is outside the glass forming region, and as a consequence, the crystallised glass-ceramics will always contain a certain volume fraction of residual glass. The degree of crystallisation in equivalent glasses formed with either yttrium or erbium after prolonged (10 h) crystallisation heat treatment at 1050°C differed; erbium resulted in 75 vol%, and yttrium in 68 vol% B-phase, see Table II and reference [14].

An increased degree of crystallisation will drain the residual glass of erbium or yttrium, and at the same time this glass will also become richer in silicon. The

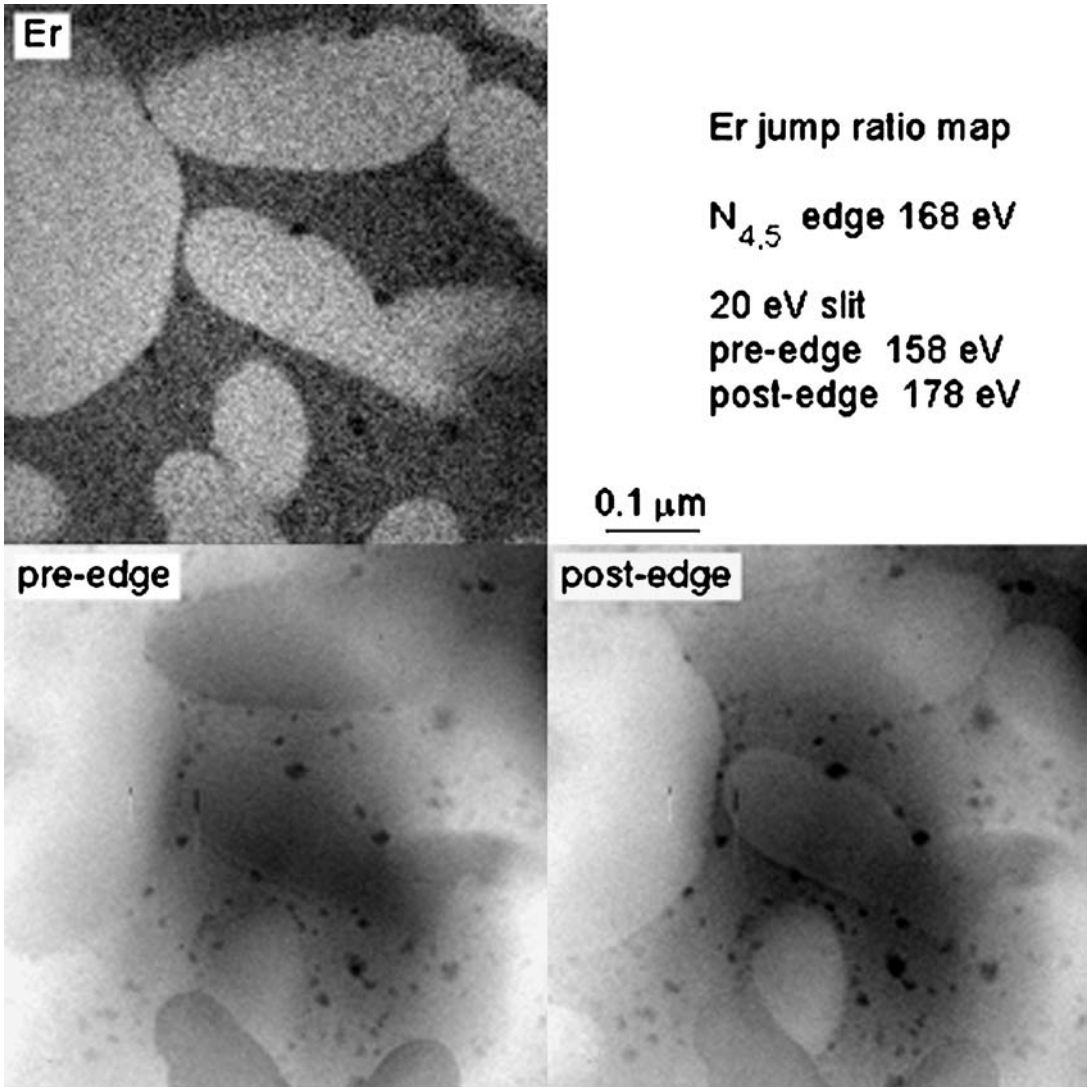

Figure 12 The computation of the erbium elemental distribution image in Fig. 11 from acquired energy filtered (pre-edge and post-edge) images.

crystallisation of B-phase will, thus, push the residual glass composition towards the Si_3N_4-SiO_2-Al_2O_3-AlN plane of the Jänecke prism as the crystallisation process proceeds. This shift in glass composition will be even more pronounced for the erbium B-phase glass-ceramic, since B-phase takes up more erbium than yttrium (Fig. 14). An altered glass composition could account for the observed phase separation in the residual glass shown in detail in Figs. 10–12. The phase separation was observed already after shorter times (1 h) at the crystallisation temperature, and became more pronounced as crystallisation proceeded. This phase separation has been observed to a limited extent in the yttrium B-phase glass-ceramic, but is even more pronounced when the equivalent ytterbium SiAlON glass is crystallisation heat treated under similar conditions [24, 27]. This difference in the extent of phase separation would be consistent with different overall residual glass compositions because of the different ranges of B-phase solid solution and different degrees of crystallisation.

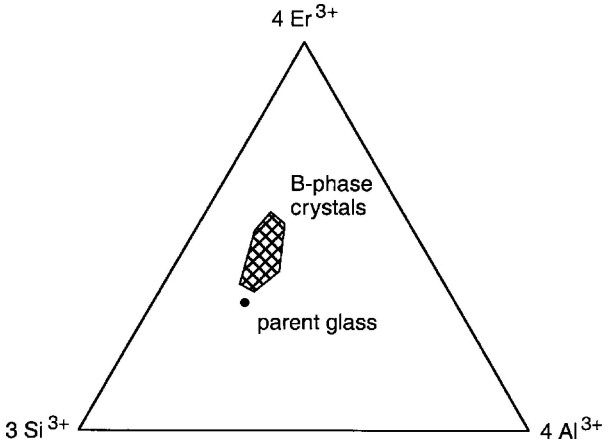

Figure 13 Triangular section of the Jänecke prism showing the range of B-phase cation composition after the crystallisation heat treatments at 1050 and 1150°C. The parent glass composition is also marked.

The anti-correlation of erbium, and aluminium, with silicon in the residual glass (Fig. 5) is in accordance with measurements on the residual glass in α-, β- and duplex α/β-sialons fabricated with the addition of Y_2O_3 or different rare earth oxides [28].

4.3. B-phase crystal size and shape

The average values of lenticular crystal diameter and thickness presented in Table I are based on

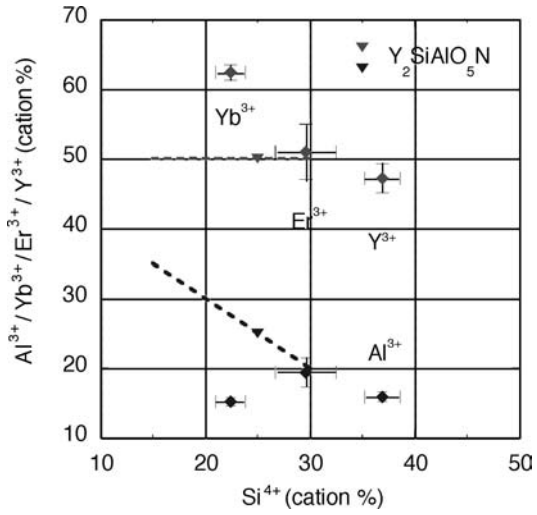

Figure 14 The average cation composition of B-phase crystals formed during crystallisation of a glass with composition (e/o) 35M:45Si:20Al:83O:17N where M = Yb, Er or Y. The data points for the Y and Yb crystals are taken from references [14, 24]. The proposed stoichiometric mid-point composition (Y_2SiAlO_5N) and solid solution range (dotted lines) of yttrium B-phase from reference [19] are also shown.

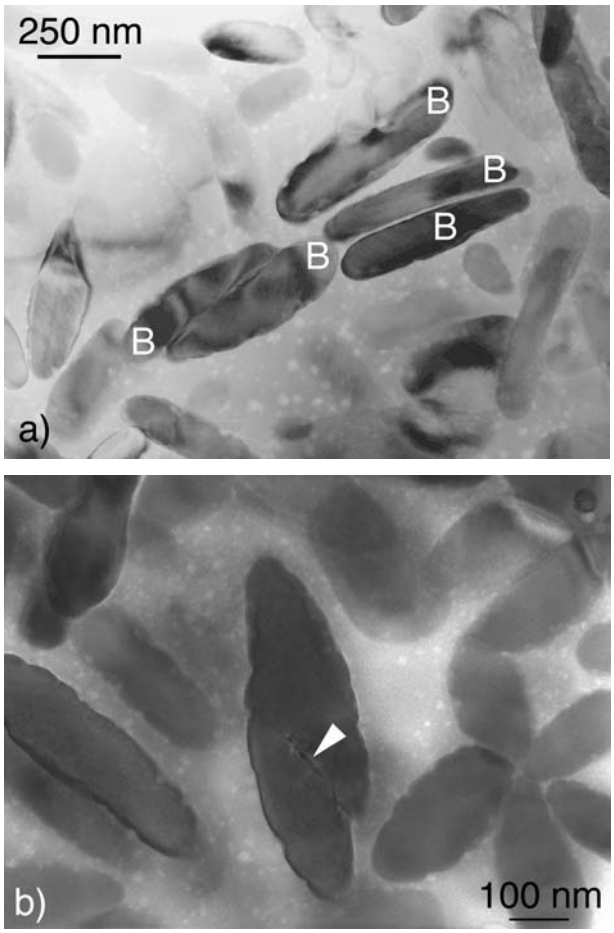

Figure 15 The alignment of adjacent B-phase crystals, marked B in (a), and their subsequent coalescence, arrowed in (b), during prolonged crystallisation heat treatment. Specimen held 10 h at 1050°C after 3 h at 948°C.

measurements of crystal section areas in TEM images that represent a section through the glass-ceramic microstructure. This section does not necessarily show the true maximum diameter and thickness of individual crystals. The large number of measurements would, however, result in representative average values. The data in Table I suggest, hence, that there are only minor variations in crystal diameter, but significant differences in crystal thickness, after the different crytallisation heat treatments at 1050°C.

The grain section measurements indicate that the nucleation time (3 or 50 h at 948°C) has only a limited effect on grain size and shape after a subsequent crystallisation heat treatment at 1050°C for 1 h, see Table I. These two materials also had the same residual glass contents. The combined results imply that any differences in glass-ceramic structure after nucleation heat treatment for different times are eliminated after a period of 1 h at a crystallisation temperature of 1050°C.

Increasing the holding time at the crystallisation temperature 1050°C, from 1 to 10 h, seems to promote growth of crystal thickness while there is only a few % change in the average crystal section diameter (Table I). This apparent change in crystal shape was accompanied by a decrease in the residual glass content, from 34 to 24%, which strongly sugggests that the increase in crystal thickness was, to some extent, caused by growth from the residual glass.

The lenticular shape taken up by the crystals in early growth is the result of a preferential growth parallel to the basal plane of the hexagonal B-phase structure, see Fig. 1. An initial rapid growth of the crystal diameter would deplete the surrounding glass in erbium, and this may slow down crystal growth. The initially significantly slower crystal growth rate in the c-direction of the hexagonal lattice (crystal thickness) suggests, however, an interface, rather than a diffusion, controlled growth of the crystal in this direction. As a result, once the freely growing lenticular crystals have reached a certain diameter, the thickness / diameter ratio would start to increase because of a reduced growth rate of the crystal diameter. This is in accordance with the results in Table I.

An increase in thickness / diameter ratio may also occur through coalescence. As shown in detail in Fig. 15, adjacent lenticular crystals tend to align, and subsequently coalesce. This phenomenon was to some extent observed also after shorter crystallisation times, but became significantly more pronounced with time at temperature. This morphology is completely different from the nucleation structure where some of the crystals appeared in pairs (or groups) around a crystalline silicon-rich feature. The crystal alignment and coalescence has been observed previously in crystallisation heat treatments of yttrium B-phase glass-ceramics [14], and also in crystallisation of the related I_w [29], but the mechanisms for this effect are still not yet well understood.

The combined EDX and EELS analyses showed an average residual glass composition of (e/o) 25Er:50Si:25Al:88O:12N after 1 h of crystallisation at 1050°C following a 3 h nucleation at 948°C. The glass residue at 1050°C may therefore be expected to be above its glass transition temperature (T_g) [8, 30]. The glass will, thus, have some fluidity and, although the viscosity would probably be rather high, the crystals will be able to move with respect to one another.

One possible mechanism for the observed alignment of crystals on top of one another, with their *c*-axis in parallel, could be due to van der Waals interactions operating across the residual glass. Such van der Waals forces depend strongly upon the dielectric properties of the crystalline and glassy phases. The layered structure of B-phase is likely to result in a significant anisotropy between directions in the (0001) basal plane and the [0001] direction. This may result in a stronger van der Waals interaction along certain crystallographic directions and thus give a driving force for neighbouring crystals to align themselves in the observed manner.

10 h at 1050°C, whithout a previous nucleation heat treatment, results in virtually the same crystal diameter but a larger crystal thickness, see Tabel I. The two structures (3 h at 948°C + 10 h at 1050°C, and 10 h at 1050°C) contain, however, the same volume fraction of residual glass. The difference in crystal shape between these two materials may, hence, be explained by an initially larger number of crystals in the nucleation heat treated material. These crystals will start to coalesce at an earlier stage in the growth process.

The occurance of crystal coalescence in prolonged crystallisation heat treatment of B-phase glass-ceramics is strongly supported by the more regular crystal shape in the material crystallised 10 h at 1150°C, see Fig. 9. It may be noted that this glass-ceramic structure contained the same volume fraction of residual glass as the materials held 10 h at the lower crystallisation temperature 1050°C (Table II).

Crystallisation heat treatment at 1050°C for 10 h of the equivalent yttrium glass, after the appropriate nucleation heat treatment, resulted in a slightly smaller apparent crystal size. The average crystal section diameter was 385 nm and the thickness 110 nm, as compared to 432 and 239 nm, respectively, for the erbium glass in the present investigation. This could possibly be explained by a more rapid diffusion of a smaller cation.

5. Conclusions

- Crystallisaton of a glass (e/o) 35Er:45Si:20Al:83O:17N occurs by the heterogeneous nucleation of lenticular B-phase crystals when heat treated at temperatures in the range 948 to 1050°C.
- Crystal growth occurs from the residual glass as well as through coalescence, where coalescence seems to dominate at prolonged crystallisaion times and at higher temperatures.
- The B-phase crystals show a wide range of composition, and the erbium is strongly anti-correlated with silicon.
- A comparison of B-phase composition after crystallisation of equivalent glasses formed with either yttrium, erbium or ytterbium show that the solid solution range depends on the yttrium or rare earth cation radius. A smaller cation radius leads to a more densely occupied cation lattice, but a more open bi-dimensional network of randomly linked (Si,Al) $(O,N)_4$ tetrahedra. As a consequence of this, the degree of crystallisation and the composition of the residual glass will, for equivalent glasses, depend on the yttrium or rare earth cation radius.
- Nitrogen:oxygen ratios from EELS indicate that B-phase is almost an oxide phase.
- The combined EDX and EELS analyses showed an average erbium B-phase formula of $Er_5Si_{3.8}Al_2O_{17}N_{0.75}$.
- The crystallisation of B-phase will push the residual glass composition towards the Si_3N_4-SiO_2-Al_2O_3-AlN plane of the Jänecke prism as the crystallisation process proceeds. This will lead to a phase separation of the glass resulting in silicon and nitrogen rich amorphous features. This process becomes more pronounced when the degree of crystallisation increases.

Acknowledgements

The other partners in the TMR NeoCeram network, Profs. D.P. Thompson, J.-L. Besson, P. Goursat, R.K. Harris, F. Cambier, and J.-C. Descamps, are thanked for their encouragement and for useful discussions. We gratefully acknowledge the provision of financial support for this work from the European Commission under the TMR Research Networks scheme, grant number: FMRX – CT96 – 0038 (DG 12 – ORGS).

References

1. R. A. L. DREW, S. HAMPSHIRE and K. H. JACK, *British Ceram. Proc.* **31** (1981) 119.
2. S. HAMPSHIRE, R. A. L. DREW and K. H. JACK, *Phys. Chem. Glasses* **26** (1985) 182.
3. R. E. LOEHMANN, *J. Am. Ceram. Soc.* **62** (1979) 491.
4. *Idem., J. Non-Cryst. Sol.* **56** (1983) 123.
5. S. HAMPSHIRE, E. NESTOR, R. FLYNN, J.- L. BESSON, T. ROUXEL, H. LEMERCIER, P. GOURSAT, M. SEBAI, D. P. THOMPSON and K. LIDDELL, *J. Euro. Ceram. Soc.* **14** (1994) 261.
6. G. LENG-WARD and M. H. LEWIS, in "Glasses and Glass-Ceramics", edited by M. H. Lewis (Chapman and Hall, London, 1990) p. 106.
7. S. SAKKA, *J. Non-Cryst. Solids* **181** (1995) 215.
8. S. HAMPSHIRE, *ibid.* **316** (2003) 64.
9. W. REDINGTON, M. REDINGTON and S. HAMPSHIRE, *Key Engng. Mater.* **206–213** (2002) 2125.
10. G. LENG-WARD and M. H. LEWIS, *Mater. Sci. Eng.* **71** (1985) 101.
11. J. L. BESSON, D. BILLIERS, T. ROUXEL, P. GOURSAT, R. FLYNN and S. HAMPSHIRE, *J. Am. Ceram. Soc.* **76** (1993) 2103.
12. H. LEMERCIER, R. RAMESH, J. L. BESSON, K. LIDDELL, D. P. THOMPSON and S. HAMPSHIRE, *Key Engng. Mater.* **132–136** (1997) 814.
13. W. T. YOUNG, L. K. L. FALK, H. LEMERCIER and S. HAMPSHIRE, *Mater. Sci. Forum* **325–326** (1999) 289.
14. W. T. YOUNG, L. K. L. FALK, H. LEMERCIER, V. PELTIER-BARON, Y. MENKE and S. HAMPSHIRE, *J. Non. Cryst. Sol.* **270** (2000) 6.
15. Y. MENKE, V. PELTIER-BARON and S. HAMPSHIRE, *British Ceram. Proc.* **60** (1999) 361.
16. I. MACLAREN, L. K. L. FALK, A. DÍAZ and S. HAMPSHIRE, *J. Am. Ceram. Soc.* **84** (2001) 1601.
17. M. F. GONON, J.-C. DESCAMPS, F. CAMBIER and D. P. THOMPSON, *Ceram. Int.* **26** (2000) 105.
18. *Idem., Mater. Sci. Forum* **325/326** (2000) 325.
19. K. LIDDELL, H. MANDAL and D. P. THOMPSON, *J. Eur. Ceram. Soc.* **17** (1997) 781.

20. S. HAMPSHIRE, H. LEMERCIER, Y. MENKE, V. PELTIER-BARON and R. RAMESH, *Turk Seramik Dernegi Yayinlari* **20** (1998) 771.
21. A. J. GUBBENS and O. L. KRIVANEK, *Ultramicroscopy* **51** (1993) 146.
22. F. HOFER, W. GROGGER, G. KOTHLEITNER and P. WARBICHLER, *ibid.* **67** (1997) 83.
23. L. K. L. FALK, *J. Eur. Ceram. Soc.* **18** (1998) 2263.
24. Y. MENKE, S. HAMPSHIRE and L. K. L. FALK, manuscript in preparation.
25. L. K. L. FALK, Y. MENKE and S. HAMPSHIRE, *Silicate Industr* **69** (2004) 119.
26. I. MACLAREN, L. K. L. FALK, A. DÍAZ and S. HAMPSHIRE, *J. Eur. Ceram. Soc.* **21** (2001) 2161.
27. W. T. YOUNG, L. K. L. FALK, Y. MENKE and S. HAMPSHIRE, unpublished.
28. L. K. L. FALK, *Ceram. Trans.* **142** (2003) 91.
29. I. MACLAREN, L. K. L. FALK, A. DIAZ and S. HAMPSHIRE, *Phil. Mag. A* **81** (2001) 867.
30. Y. MENKE, V. PELTIER-BARON and S. HAMPSHIRE, *J. Non. Cryst. Sol.* **276** (2000) 145.

Received 9 December 2004
and accepted 9 May 2005